

Strong slowing down of water reorientation in mixtures of water and tetramethylurea

Y. L. A. Rezus* and H. J. Bakker

*FOM-institute for Atomic and Molecular Physics,
Kruislaan 407, 1098 SJ Amsterdam, The Netherlands*

Abstract

We use mid-infrared pump-probe spectroscopy to study the ultrafast dynamics of HDO molecules in mixtures of tetramethylurea (TMU) and water. The composition of the studied solutions ranges from pure water to an equimolar mixture of water and TMU. We find that the vibrational relaxation of the OD-stretching vibration of HDO proceeds via an intermediate level in which the molecule is more strongly hydrogen bonded than in the ground state. As the TMU concentration is increased, the lifetime of the excited state and of the intermediate increase from 1.8 ps to 5.2 ps and from 0.7 ps to 2.2 ps, respectively. The orientational relaxation data indicate that the solutions contain two types of water molecules: bulk-like molecules that have the same reorientation time constant as in the pure liquid ($\tau_{\text{rot}} = 2.5$ ps) and molecules that are strongly immobilized ($\tau_{\text{rot}} > 10$ ps). The immobilized water molecules turn out to be involved in the solvation of the methyl groups of the tetramethylurea molecule. The fraction of immobilized water molecules grows with increasing TMU concentration, reaching a limiting value of 60% at very high concentrations.

Keywords: Ultrafast spectroscopy, hydrogen bonds, orientational dynamics, hydrophobic solvation

I. INTRODUCTION

Liquid water possesses many remarkable properties and, as such, has become a research topic in many scientific fields: in chemistry and biology it forms the universal solvent, which dissolves salts, allows biochemical reactions to take place and mediates the folding of proteins; in physics, liquid water is the number one example of a complex fluid, in which cooperative effects and many-body interactions play an important role. The special properties of water are the consequence of its structure: it consists of a highly dynamic, three-dimensional network, in which most water molecules are connected to four neighbors. In the past decade mid-infrared pump-probe spectroscopy has proven itself to be a powerful tool for studying the structure and dynamics of the hydrogen-bond network of water, and the technique has provided considerable insight into the various types of fluctuations and structural dynamics that are present in this network.¹⁻⁶ In addition to being used for the study of the pure liquid, mid-infrared pump-probe spectroscopy has also been used to study a variety of systems in which the hydrogen-bond network of water is, to greater or lesser extent, perturbed, such as water confined in reverse micelles, aqueous salt solutions, and organic solvents containing clusters and complexes of water molecules.⁷⁻¹¹

In a recent study we investigated the effect of urea on the structural dynamics of the hydrogen-bond network of water.¹² Surprisingly, we found that the presence of urea does not affect the dynamics of the water molecules in aqueous solutions of urea, not even at extremely high concentrations (12 mol/kg). This finding led us to conclude that urea fits into the hydrogen-bond network of water exceptionally well, and we attributed this to urea's ability of forming no less than eight hydrogen bonds with water. The exceptional hydrogen-bonding capabilities of urea cause the urea-water interactions to be very similar to water-water interactions, which explains the ideal behavior of aqueous urea. Considering these results it would be very interesting to restrict the hydrogen-bonding possibilities of urea and to investigate how this affects the hydrogen-bond network of water. For this purpose we have chosen to study a derivative of urea, in which the amine hydrogens are substituted by methyl groups. The thus formed molecule, tetramethylurea (TMU), is highly soluble in water, so that aqueous solutions of it can be studied over a wide concentration range.¹³⁻¹⁵

In this article we present measurements of the ultrafast dynamics of HDO molecules in mixtures of water and TMU over a wide range of concentrations, which range from pure

water to nearly pure TMU. These measurements shed light on the vibrational relaxation mechanism of the OD vibration of HDO, and they provide information on the solvation structure of hydrophobic groups in water.

II. EXPERIMENTAL METHODS

The laser system used in our experiments consists of a commercial Ti:sapphire regenerative amplifier that delivers 800-nm pulses with a duration of 100 fs and an energy of 1 mJ. Approximately 70% of this light is used to pump an optical parametric amplifier (OPA) based on β -barium borate (BBO). The OPA is tuned to produce idler pulses with a wavelength of 2.0 μm . These pulses are frequency doubled in a second BBO crystal and subsequently difference-frequency mixed in a KNbO_3 crystal using the 800-nm light (30%) that was split off before the OPA. This process yields mid-infrared pulses that are resonant with the OD-stretch vibration, having a wavelength of 4 μm and an energy of a few μJ .

The mid-infrared light thus obtained is coupled into a pump-probe setup. A wedged CaF_2 window is used to split off broadband probe and reference pulses. The probe light is directed onto a retroreflector that is mounted on a computer-controlled delay stage. The transmitted light forms the pump beam, and, using a $\lambda/2$ -plate its polarization is set to 45 degrees with respect to that of the probe beam. The pump, probe and reference beams are focused onto the sample using an off-axis parabolic mirror, and they are recollimated by an identical mirror that is placed after the sample. The probe and reference beams are focused onto the entrance slit of a spectrometer, which disperses the beams onto a 2x32 liquid-nitrogen-cooled mercury-cadmium-telluride (MCT) array. Before entering the spectrometer, the probe beam passes through a polarizer allowing the selection of either its parallel or perpendicular polarization component with respect to the pump polarization. The polarizer is rotated using a motorized rotational stage. The polarization selection results in the transient absorptions $\Delta\alpha_{\parallel}(\omega, t)$ and $\Delta\alpha_{\perp}(\omega, t)$, respectively. From these signals we construct the isotropic signal, which is independent of orientational processes,

$$\Delta\alpha_{\text{iso}}(\omega, t) = \frac{\Delta\alpha_{\parallel}(\omega, t) + 2\Delta\alpha_{\perp}(\omega, t)}{3}. \quad (1)$$

We use the same two signals to construct the anisotropy, which is independent of vibrational

relaxation and only reflects reorientation,

$$R(\omega, t) = \frac{\Delta\alpha_{\parallel}(\omega, t) - \Delta\alpha_{\perp}(\omega, t)}{3\Delta\alpha_{\text{iso}}}. \quad (2)$$

Our samples consist of mixtures of TMU and water. Since we study mixtures over a wide composition range, we do not use the TMU concentration to specify the composition, but we rather use the symbol w , which represents the number of TMU molecules present in the solution per water molecule,

$$w = \frac{[\text{TMU}]}{[\text{H}_2\text{O}]}. \quad (3)$$

To the water we have added 4% of heavy water (D_2O), and as a consequence 8% of the water is present as HDO molecules. The low HDO concentration ensures that no resonant intermolecular energy transfer occurs between different HDO molecules. The thickness of our samples varies between 25 μm and 200 μm and is chosen such that an optical density of ~ 1 is obtained. The sample cell consists of two CaF_2 windows held apart by a teflon spacer of appropriate thickness.

III. RESULTS AND INTERPRETATION

A. Linear spectra

Figure 1 displays the linear spectra of HDO in pure H_2O and in two solutions of TMU. The water-TMU background was subtracted from these spectra, so that they only display the absorption due to the HDO molecules. The frequency region shown corresponds to the absorption by the OD-stretching vibration. A blueshift of the band is observed with increasing TMU concentration, which is indicative of a decrease of the average hydrogen-bond strength in the network of water molecules.¹⁶ However, we note that very high concentrations are needed to cause a significant weakening of the hydrogen-bond network: for the solution with $w = 0.2$, corresponding to only five water molecules per TMU molecule, only a small shift is observed. Apparently the hydrogen-bond network of water can accommodate the TMU molecules without being significantly perturbed. A considerable weakening of the hydrogen bonds only occurs for concentrations that are so high that they prevent the formation of a connected network of water molecules.

B. Isotropic transient spectra

Figure 2 shows transient spectra for a TMU solution with $w = 0.1$. The spectra at 0.5 ps and 2 ps display a decreased absorption around 2500 cm^{-1} due to the bleaching of the fundamental transition. For frequencies $<2430\text{ cm}^{-1}$ an increased absorption is observed, which is due to the absorption of the excited vibrational state. Vibrational relaxation causes the amplitude of the transient spectrum to decrease with increasing pump-probe delay; nevertheless, at 20 ps a non-zero, residual absorption change is observed that persists without decay over the experimentally accessible time range (~ 500 ps). This long-time absorption change is caused by the temperature increase in the sample that arises from the absorption and subsequent thermalization of the energy of the pump pulse. Since a temperature increase shifts the OD band to the blue, the long-time absorption change consists of an induced absorption on the blue side of the spectrum and a bleach on the red side.

In figure 3 we have plotted delay scans for different frequencies in the transient spectrum of figure 2. The top and bottom panel show a bleach and an induced absorption, respectively, that decay on a ~ 2 ps timescale. The middle panel shows a delay scan at an intermediate frequency that displays more complicated behavior. Here a competition is observed between a decaying bleach and an ingrowing heating signal, which is a bleach at this frequency. The fact that the signal turns over indicates that the heating is delayed with respect to the relaxation of the OD vibration, as has been described in previous work on the relaxation of HDO in pure water.¹⁷ However, this explanation does not yet account for one aspect of the considered signal, that is to say, the fact that the signal rises temporarily above zero: an induced absorption cannot arise from the sum of two contributions that both have the character of a bleach. We shall return to this issue when discussing the relaxation mechanism of the OD vibration.

In order to describe the time-dependence of the transient spectra of HDO in solutions of TMU, we turn to the mechanism that describes the relaxation of HDO in pure water.¹⁷ This mechanism is depicted in figure 4. The first step in the relaxation is the decay of the excited OD vibration to an intermediate level. This transfer occurs with a rate constant k_1 ($1/\tau_1$). Subsequently the intermediate level decays to the ground state (with a rate constant $k_* = 1/\tau_*$), which is accompanied by thermalization of the vibrational energy. As a consequence the temperature rises, and the spectrum shifts to the blue. This spectral shift

is incorporated in the model by attributing a different spectrum to the heated ground state (0') than to the ground state (0). The spectra of the different transitions are denoted by the symbols σ_{01} , σ_{12} , σ_{01}^* and σ'_{01} .

The absorption change that follows from this relaxation model is given by

$$\begin{aligned}\Delta\alpha(\omega, t) &= N_1(t)\sigma_{12}(\omega) - [N_1(0) + N_1(t)]\sigma_{01}(\omega) + N_0^*(t)\sigma_{01}^*(\omega) + N_0'(t)\sigma'_{01}(\omega), \\ &= N_1(t)\sigma_{12}(\omega) + [-N_1(0) - N_1(t) + N_0^*(t) + N_0'(t)]\sigma_{01}(\omega) \\ &\quad + \Delta\sigma'_{01}(\omega)N_0'(t) + \Delta\sigma_{01}^*(\omega)N_0^*(t).\end{aligned}\tag{4}$$

where $\Delta\sigma'_{01} = \sigma'_{01} - \sigma_{01}$ and $\Delta\sigma_{01}^* = \sigma_{01}^* - \sigma_{01}$.²⁴ The expressions for the populations can be obtained by solving the rate equations that correspond to the relaxation mechanism in figure 4. These expressions are listed in appendix A. By substituting for the populations we arrive at the following expression

$$\begin{aligned}\Delta\alpha(\omega, t)/N_1(0) &= \{\sigma_{12}(\omega) - 2\sigma_{01}(\omega)\}e^{-k_1t} + \Delta\sigma'_{01}(\omega)\left\{\frac{k_1}{k_* - k_1}e^{-k_*t} - \frac{k_*}{k_* - k_1}e^{-k_1t} + 1\right\} \\ &\quad + \Delta\sigma_{01}^*(\omega)\frac{k_1}{k_* - k_1}\left(e^{-k_1t} - e^{-k_*t}\right).\end{aligned}\tag{5}$$

This expression consists of three terms. The first term represents the combined bleaching of the fundamental transition and induced absorption of the excited state; the second term represents the ingrowing heating signal; finally, the last term is a correction for the fact that the intermediate state may have a spectrum that is different from that of the ground state. In previous work on HDO in H₂O this term was neglected because it was assumed that $\Delta\sigma_{01}^* = 0$.

For each TMU solution a fit of equation 5 to the time-dependent transient spectrum has been performed. Hereby the frequency-dependent cross-sections, $\sigma_{12}(\omega) - 2\sigma_{01}(\omega)$, $\Delta\sigma'_{01}(\omega)$ and $\Delta\sigma_{01}^*(\omega)$, were allowed to vary freely. Thus each time-dependent transient spectrum is characterized by three cross-section spectra and two rate constants (k_1 and k_*). In figures 2 and 3 the solid lines show the resulting fit for the $w = 0.1$ solution. It can be seen that this relaxation model provides an excellent description of the data. For the other solutions the fits are of similar quality, indicating that the relaxation mechanism does not change as the composition of the solution is varied. The two relaxation time constants, however, do vary, and they both increase as the TMU concentration is increased (figure 5); τ_1 increases from 1.8 ps to 5.2 ps and τ_* increases from 0.7 ps to 2.2 ps. This reflects the slowing down of the

vibrational relaxation of the HDO molecule upon truncation of the hydrogen-bond network of water.

From the fit we obtain the time-dependent populations of the three levels in the relaxation. We have plotted these populations in figure 6 for the $w = 0.1$ solution. We recognize the mono-exponentially decaying excited state and the heated ground state that grows in bi-exponentially. The intermediate state starts with no population at $t = 0$, becomes populated up to a maximum, and subsequently tracks the decay of the excited state. The population dynamics are qualitatively similar for the other solutions.

Apart from the populations the fits also provide us with the spectral shapes that correspond to these three populations. We have plotted these spectral components in figure 7 for three TMU solutions. The spectral shape corresponding to the excited state population resembles the transient spectrum at short delay, as is to be expected from the fact that at these delays only the excited state is populated. Similarly, the spectrum of the heated ground state is identical to the transient spectrum at long delays. For the intermediate state, however, we observe a spectrum that cannot be inferred directly from the data. The spectral shape of $\Delta\sigma_{01}^*$ shows that at all frequencies the intermediate state has an increased absorption in comparison to the ground state. As far as the heating spectrum is concerned, we note that its amplitude decreases relative to that of the two other spectra as the TMU concentration is increased. This is explained by the fact that the sample thickness was increased upon increasing the TMU concentration, in order to maintain the same optical density by HDO. Since the pump energy is thus spread over a larger volume, the resulting temperature jump decreases in magnitude.

As was mentioned above, in previous work on the relaxation of the OD vibration of HDO the spectrum of the intermediate state was assumed to be the same as that of the ground state. Indeed, we find that at low TMU concentrations the transient spectra of the TMU solutions can very well be fit using only the first two terms in equation 5. At high TMU concentrations, however, this is no longer possible. The reason why two spectral components suffice at low concentrations is that the heating signal can to some extent compensate for the spectral component associated with the intermediate state. At high TMU concentrations the heating signal decreases in amplitude, so that it can no longer play this role. The increased absorption of the intermediate level also explains the overshoot to positive values observed in the delay scan in the middle panel of figure 3. In fact, the overshoot unambiguously proves

the necessity of introducing the intermediate-state spectrum into the relaxation model, and it rules out the possibility that the spectrum is merely a fitting artifact.

We would like to stress that the increased absorption of the intermediate state is a general feature of the relaxation pathway of the HDO molecule, which is independent of the solvent (be it pure H₂O or aqueous TMU). The effect of the intermediate state is only more clearly observed for samples in which the HDO molecules are effectively diluted, so that the thermal effect is diminished. The reason that it is difficult to observe the effect for HDO in pure H₂O is that one cannot use thick samples because of the relatively strong background absorption at $\sim 2500\text{ cm}^{-1}$ of the H₂O solvent.

C. Anisotropy dynamics

As is clear from the discussion above, the measured absorption change does not solely reflect the dynamics of the excitation but also contains an additional contribution due to heating. This contribution is isotropic in nature, and it overshadows the excitation dynamics for long pump-probe delays. Therefore it is necessary to subtract this contribution from both $\Delta\alpha_{\parallel}$ and $\Delta\alpha_{\perp}$ before using these quantities to calculate the anisotropy (equation 2). The fit to the relaxation model provides us with the necessary information about the dynamics of the heating signal, so that we can perform this correction unambiguously at all delay times.

In figure 8 we have plotted the calculated anisotropy decays for a few TMU solutions of different composition. The probe frequencies correspond to the peak position of the bleach. We observe biexponential decays with a fast decay time of $\sim 2.5\text{ ps}$ and a slow component that cannot be fully resolved but that has a time constant $>10\text{ ps}$. The fast time constant does not show any significant variation with solution composition (figure 9a); a slight increase is only observed for the most concentrated solution. The value of 2.5 ps for this time constant is identical to the reorientation time of HDO in pure water.¹⁷ In order to investigate the origin of the slow component, we turn to the concentration dependence of its amplitude. In figure 9b we have plotted the amplitude of the slow component versus the solution composition. We observe a strong variation of the amplitude that is linear at low concentrations ($w < 0.05$) and flattens at high concentrations.

These observations indicate that the water molecules in a TMU solution are partitioned into two fractions. One fraction is composed of bulk-like water molecules that display

the same orientational dynamics as in the pure liquid; the other fraction consists of water molecules that are strongly immobilized, in the sense that they display much slower orientational dynamics than the bulk water molecules. The linear variation of the immobilized fraction at low concentrations demonstrates that these molecules are to be associated with the solvation shell of a TMU molecule. Consequently, the upper limit for the reorientation time of these immobilized water molecules is given by the reorientation time of the TMU solute. From the slope of the linear part of the graph in figure 9b we calculate that every TMU molecule is responsible for the immobilization of 15 ± 2 water OH groups. At high concentrations the solvation shells of different TMU molecules overlap, which explains the deviation from linear behavior observed at these concentrations. At very high concentrations saturation is observed at a value of the anisotropy of 0.25, from which we conclude that 60% of all water molecules are immobilized in these solutions.

In figure 10 we compare the anisotropy decay on the red side of the spectrum with that on the blue side for two solutions: one with a low TMU concentration and one with a high concentration. For the low TMU concentration we see practically no difference between the anisotropy decays on the red and blue side of the spectrum. This observation is in agreement with studies of HDO in pure water, which showed no dependence of the anisotropy decay on the probe wavelength.^{2,17} For the concentrated solution corresponding to $w = 1$, however, we observe that the anisotropy decays faster on the blue side of the spectrum than on the red side. This spectral dependence of the anisotropy reflects the heterogeneity in the local environments of water molecules, that apparently occurs in highly concentrated solutions of TMU.

IV. DISCUSSION

We have shown that the relaxation of the OD vibration of HDO proceeds through an intermediate level that has an increased absorption relative to the ground state. However, the nature of this state has not yet been specified. It is reasonable to assume that the intermediate state is a state in which a low-frequency mode is excited and that this excitation affects the frequency and cross-section of the ground-state spectrum of the OD vibration via an anharmonic interaction. The spectral shape of $\Delta\sigma_{01}^*$ shows an increased absorption in the center and on the red side of the spectrum. A possible explanation for this observation

could be that the vibrational relaxation of the OD vibration leads to the excitation of the hydrogen-bond stretching vibration. The excitation of this low-frequency vibration results in a broadening of the hydrogen-bond length distribution. Because the cross-section of the OD vibration increases strongly when the hydrogen-bond strength increases (and therefore when moving to the low-frequency side of the spectrum), this broadening will primarily lead to an increase in the spectral intensity on the red side of the spectrum.

As was mentioned in the introduction we recently investigated the effect of urea on the structural dynamics of water.¹² We found that, up to the highest concentrations studied (12 mol/kg), urea did not have any effect on the orientational dynamics of the majority of the water molecules. A small fraction of the water molecules, however, displayed much slower dynamics, similar to what is observed here for TMU. However, the effect was a lot smaller for urea than it is for TMU: only 1 OH group is immobilized per urea molecule, whereas 15 ± 2 OH groups are immobilized per TMU molecule. The immobilized water fraction in aqueous urea was attributed to the presence of water molecules that are doubly hydrogen bonded to urea: a single water molecule donates a hydrogen bond to the carbonyl oxygen, and it simultaneously accepts one from the amine cis-hydrogen. Clearly, TMU cannot engage in this type of hydrogen bonding with water. As TMU differs with urea only in the substitution of the amine hydrogens by methyl groups, it is clear that the methyl groups play an important role in the immobilization of water molecules in solutions of TMU.

We now turn to the physical mechanism by which the methyl groups of TMU may cause the immobilization of water molecules around themselves. It is clear that direct interactions between water and the methyl groups of TMU cannot be held responsible for this effect, since the apolar methyl groups interact only weakly with the polar water molecules. As was discussed above, the effect can neither be attributed to a strengthening of the hydrogen bonds between the water molecules themselves; on the contrary, the linear spectrum indicates that the average hydrogen-bond strength decreases with an increase in the TMU concentration.

A number of molecular dynamics studies on liquid water have appeared in the past years that shed light on this issue. Sciortino et al. have shown that the relatively high orientational mobility of pure water is related to the presence of defects (i.e. five-coordinated water molecules) in the tetrahedral hydrogen-bond network of liquid water.¹⁸ They have suggested that the slowing down of water dynamics around hydrophobic groups is the consequence of a steric effect, which prevents the creation of five-coordinated water molecules around

these groups. Recently Laage and Hynes proposed a detailed mechanism for the reorientation of water in which five-coordinated water molecules play an important role.¹⁹ These authors demonstrated that the pathway for reorientation involves a rotating water molecule that concertedly breaks a hydrogen bond with an overcoordinated first-shell neighbor and reforms one with an undercoordinated second-shell neighbor. In another molecular dynamics study by Sharp et al. the effect of hydrophobic solutes on the structure of water was investigated.²⁰ These researchers observed that hydrophobic solutes tend to preferentially displace water molecules that overcoordinate a second water molecule, providing a rationale for why hydrophobic solutes lower the amount of network defects. These studies together with our results form compelling evidence for the notion that the immobilization of water molecules around the methyl groups of TMU arises from a steric effect, in which the methyl groups prevent a fifth water molecule from approaching a tetrahedrally coordinated water molecule, and as such prevents the molecule to reorient.

The presence of a hydration shell around TMU that contains strongly immobilized water molecules was recently also observed for other molecules containing hydrophobic groups.²¹ In fact this observation provides support for the theory by Frank and Evans that was used to explain the thermodynamic anomalies of the dissolution of hydrophobic compounds in water.²² These researchers suggested that hydrophobic solutes are solvated by patches of water molecules possessing an increased ordering, somewhat resembling the structure of ice. Here we have shown that such a distinct solvation shell indeed exists and that it is ice-like, but only from the perspective of its orientational dynamics; its structure, on the other hand, as inferred from the hydrogen-bond strength, should rather be regarded as water-like.

At high TMU concentrations the anisotropy becomes dependent on the probe frequency, decaying faster on the blue side of the spectrum than on the red side (figure 10b). This observation points to the existence of structures in the hydrogen-bond network that are relatively long-lived and do not interconvert on a 10 ps timescale. Below we investigate the nature of these structures.

At high TMU concentrations the amplitude of the slow component in the anisotropy displays an asymptotic behavior as a function of the TMU concentration. The fact that the limiting value is practically reached at a composition of $w = 0.2$ suggests that beyond this concentration the average environment of a water molecule no longer changes with increasing TMU concentration. A priori one can envision two possibilities for the structure

of these solutions, which contain an excess volume of TMU: either the water is present as isolated water molecules, hydrogen bonded to TMU, or it is present as clusters of water molecules. Let us consider the first possibility and see whether it can explain the observed anisotropy dynamics. Water molecules that are present as isolated molecules are likely to have one OH group that is hydrogen bonded to TMU and another that is dangling in a hydrophobic environment. In this situation the slow component in the reorientation would be the consequence of the hydrogen-bonded OH groups and the fast component would be caused by the unbound OH groups. However, since a carbonyl group can only bind two water molecules, it is difficult to understand how this behavior can already set in at a composition of $w = 0.2$, corresponding to five water molecules per TMU molecule. Therefore, the option that the water is present as water clusters seems more plausible. This structure accounts for the fact that the environment of a water molecule remains the same beyond a certain TMU concentration. Moreover, molecular dynamics simulations have shown that water indeed forms clusters in hydrophobic cavities.²³ The immobilization of water molecules in these clusters is likely to proceed through a mechanism that resembles the mechanism in dilute TMU solutions. That is, the immobilized OH groups are located in the vicinity of the methyl groups and cannot be approached by a new hydrogen-bonding partner; water molecules in the interior of the cluster are responsible for the fast reorientation because of their ability to become fivefold coordinated. However, there is another type of OH group that we need to consider. Due to the finite size of a cluster not all water molecules can form four hydrogen bonds, so that there will also be unbound OH groups, which are mobile. We conclude that at high TMU concentration the mobile OH fraction contains both hydrogen bonded OH groups and unbound OH groups. The unbound OH groups absorb on the blue side of the spectrum; as a consequence the mobile fraction is largest in this frequency region, resulting in a lower end level in the anisotropy (figure 10b).

V. CONCLUSIONS

We studied the vibrational relaxation and orientational dynamics of HDO molecules in aqueous solutions of tetramethylurea (TMU), the composition of which varied from pure water to an equimolar mixture of water and TMU. The vibrational relaxation of the OD vibration of HDO was found to proceed via an intermediate level in which the HDO molecule

is more strongly hydrogen bonded than in the ground state. This aspect of the intermediate level also applies for HDO in pure water, but it was not previously observed because the effect was always obscured by a strong heating signal. When increasing the TMU concentration the lifetimes of the excited state and of the intermediate state increase from 1.8 ps to 5.2 ps and 0.7 ps to 2.2 ps, respectively.

By studying the orientational dynamics we discovered that the water molecules in these solutions are partitioned into two fractions: one fraction displays bulk-like dynamics and reorients with the same time constant as in the bulk liquid ($\tau_{\text{rot}} = 2.5$ ps); the other fraction is immobilized and displays much slower orientational dynamics ($\tau_{\text{rot}} > 10$ ps). The immobilized fraction turns out to be part of the hydrophobic hydration shell of the TMU molecule, and we found that at low concentrations every TMU molecule immobilizes 15 ± 2 water OH groups. The immobilization of water molecules is the consequence of a steric effect in which the methyl groups hinder the formation of network defects in the hydrogen-bond network of water; since these network defects are known to catalyze the reorientation of water molecules, their absence explains the observed immobilization. At high TMU concentrations the structure of the solution becomes heterogeneous with the water molecules present in the form of clusters in the TMU matrix.

APPENDIX A: EQUATIONS FOR VIBRATIONAL RELAXATION

The populations of the three levels in the relaxation mechanism shown in figure 4 obey the following set of differential equations

$$\begin{aligned} \frac{dN_1}{dt} &= -k_1 N_1, \\ \frac{dN_0^*}{dt} &= k_1 N_1 - k_* N_0^*, \\ \frac{dN_0'}{dt} &= k_* N_0^*. \end{aligned} \tag{A1}$$

These equations can be integrated successively to yield the following expressions for the populations,

$$\begin{aligned} N_1(t)/N_1(0) &= e^{-k_1 t}, \\ N_0^*(t)/N_1(0) &= \frac{k_1}{k_* - k_1} \left(e^{-k_1 t} - e^{-k_* t} \right), \\ N_0'(t)/N_1(0) &= \frac{k_1}{k_* - k_1} e^{-k_* t} - \frac{k_*}{k_* - k_1} e^{-k_1 t} + 1. \end{aligned} \tag{A2}$$

-
- * Electronic address: rezus@amolf.nl
- ¹ J. J. Loparo, C. J. Fecko, J. D. Eaves, S. T. Roberts, and A. Tokmakoff, *Phys. Rev. B* **70**, 180201 (2004).
 - ² T. Steinel, J. B. Asbury, J. Zheng, and M. D. Fayer, *J. Phys. Chem. A* **108**, 10957 (2004).
 - ³ J. Stenger, D. Madsen, P. Hamm, E. T. J. Nibbering, and T. Elsaesser, *J. Phys. Chem. A* **106**, 2341 (2002).
 - ⁴ J. Lindner, P. Vohringer, M. S. Pshenichnikov, D. Cringus, D. A. Wiersma, and M. Mostovoy, *Chem. Phys. Lett.* **421**, 329 (2006).
 - ⁵ A. J. Lock and H. J. Bakker, *J. Chem. Phys.* **117**, 1708 (2002).
 - ⁶ M. L. Cowan, B. D. Bruner, N. Huse, J. R. Dwyer, B. Chugh, E. T. J. Nibbering, T. Elsaesser, and R. J. D. Miller, *Nature* **434**, 199 (2005).
 - ⁷ A. M. Dokter, S. Woutersen, and H. J. Bakker, *Phys. Rev. Lett.* **94**, 178301 (2005).
 - ⁸ H. S. Tan, I. R. Piletic, and M. D. Fayer, *J. Chem. Phys.* **122**, 174501 (2005).
 - ⁹ D. Cringus, S. Yeremenko, M. S. Pshenichnikov, and D. A. Wiersma, *J. Phys. Chem. B* **108**, 10376 (2004).
 - ¹⁰ J. J. Gilijamse, A. J. Lock, and H. J. Bakker, *Proc. Natl. Acad. Sci. U.S.A* **102**, 3202 (2005).
 - ¹¹ M. F. Kropman, H.-K. Nienhuys, and H. J. Bakker, *Phys. Rev. Lett.* **88**, 077601 (2002).
 - ¹² Y. L. A. Rezus and H. J. Bakker, *Proc. Natl. Acad. Sci. U.S.A* **103**, 18417 (2006).
 - ¹³ U. Kaatze, H. Gerke, and R. Pottel, *J. Phys. Chem.* **90**, 5464 (1986).
 - ¹⁴ V. Y. Bezzabotnov, L. Cser, T. Grosz, G. Jancso, and Y. M. Ostanovich, *J. Phys. Chem.* **96**, 976 (1992).
 - ¹⁵ G. Jakli and W. A. V. Hook, *J. Chem. Eng. Data* **46**, 777 (2001).
 - ¹⁶ W. Mikenda, *J. Mol. Struct.* **147**, 1 (1986).
 - ¹⁷ Y. L. A. Rezus and H. J. Bakker, *J. Chem. Phys.* **123**, 114502 (2005).
 - ¹⁸ F. Sciortino, A. Geiger, and H. E. Stanley, *Nature* **354**, 218 (1991).
 - ¹⁹ D. Laage and J. T. Hynes, *Science* **311**, 832 (2006).
 - ²⁰ K. R. Gallagher and K. A. Sharp, *J. Am. Chem. Soc.* **125**, 9853 (2003).
 - ²¹ Y. L. A. Rezus and H. J. Bakker, *Phys. Rev. Lett.* **99**, 148301 (2007).
 - ²² H. S. Frank and M. W. Evans, *J. Chem. Phys.* **13**, 507 (1945).

²³ S. Vaitheeswaran, H. Yin, J. C. Rasaiah, and G. Hummer, Proc. Natl. Acad. Sci. U.S.A **101**, 17002 (2004).

²⁴ Strictly speaking, it is not physically correct to model the heating signal via a heated ground state. The reason is that this approach implicitly attributes the absorption change due to heating to only the relaxed HDO molecules. In reality, however, the temperature increase is experienced by all HDO molecules (irrespective of whether they had been excited or not), so that they all contribute to the heating signal. A more physical way of modelling the heating is to incorporate the absorption change due to the increased temperature into a time-dependent $\sigma_{01}(\omega, t)$. However, it was previously shown that this approach leads to a heating term that is identical to the one in equation 5 except for a correction factor $(1 - Fe^{-k_1t})$ where F is the fraction of excited HDO molecules.¹⁷ Since this fraction does not exceed a few percent, it can be safely ignored.

ACKNOWLEDGMENTS

This work is part of the research program of the “Stichting voor Fundamenteel Onderzoek der Materie (FOM)”, which is financially supported by the “Nederlandse organisatie voor Wetenschappelijk Onderzoek (NWO)”.

FIGURES

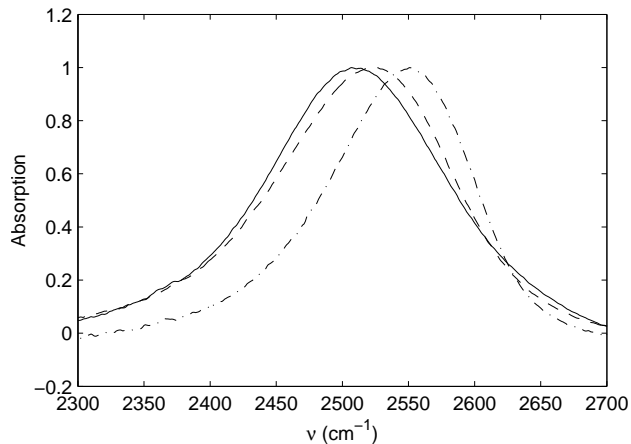


FIG. 1: Linear spectra of HDO in H₂O with different amounts of added tetramethylurea. The spectra are corrected for the H₂O and TMU background so that only the absorption due to the HDO molecule is visible. The solid line refers to the spectrum corresponding to $w = 0$ (HDO in H₂O), the dashed line to $w = 0.2$ and the dashed-dotted line to $w = 1$.

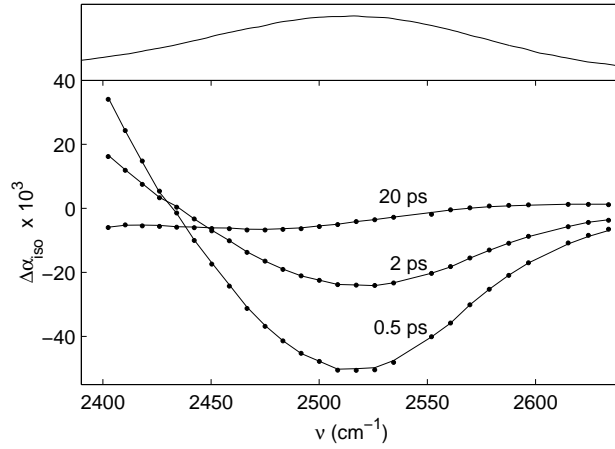


FIG. 2: Transient spectra (dots) of a solution of TMU in HDO/H₂O corresponding to $w = 0.1$ at delays of 0.5, 2 and 20 ps. The solid line represents a fit to the relaxation model described in the text. The top panel shows the linear spectrum.

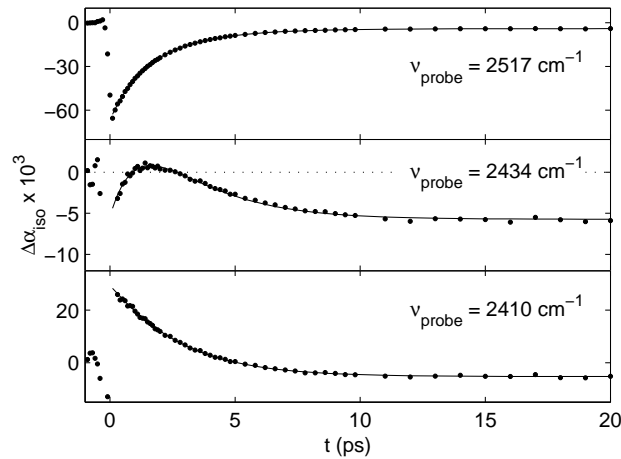


FIG. 3: Delay scans for a TMU solution corresponding to $w = 0.1$ at different probe frequencies. The dots represent the experimental data points and the solid line is the fit to the relaxation model described in the text.

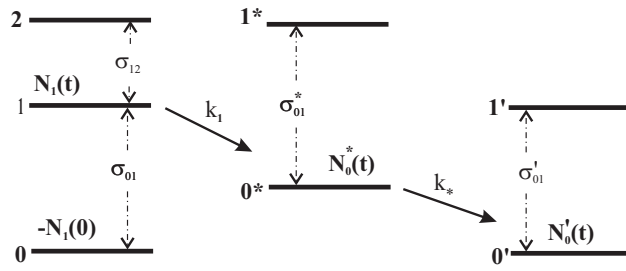


FIG. 4: Model used to describe the relaxation of the OD vibration of the HDO molecule in aqueous TMU solutions. The excited state first decays to an intermediate state that has a different spectrum than the ground state. The subsequent decay of this level leads to thermalization of the vibrational energy and, as such, to heating of the sample.

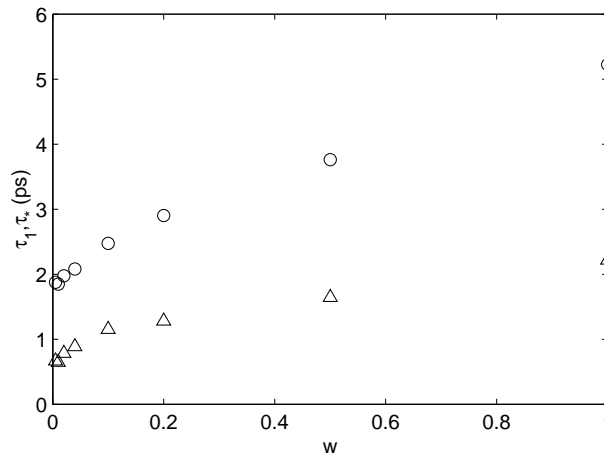


FIG. 5: Relaxation times of the OD vibration of HDO as a function of the composition of the solution. The circles represent τ_1 and the triangles τ_* .

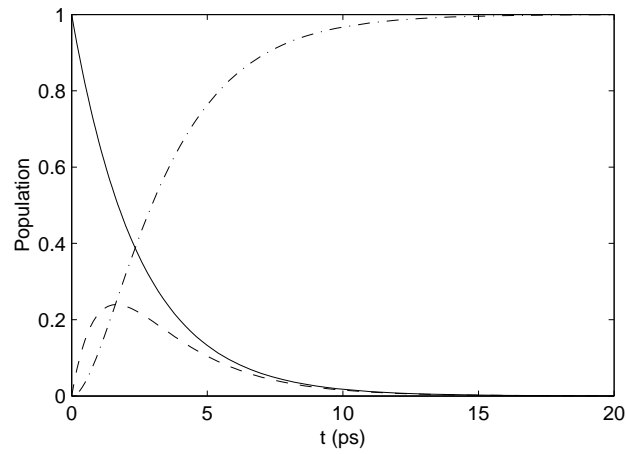


FIG. 6: Populations of the three states in the relaxation model for the TMU solution with $w = 0.1$. The solid line is the excited state population, the dashed line the intermediate state population, and the dashed-dotted line represents the population of the heated ground state.

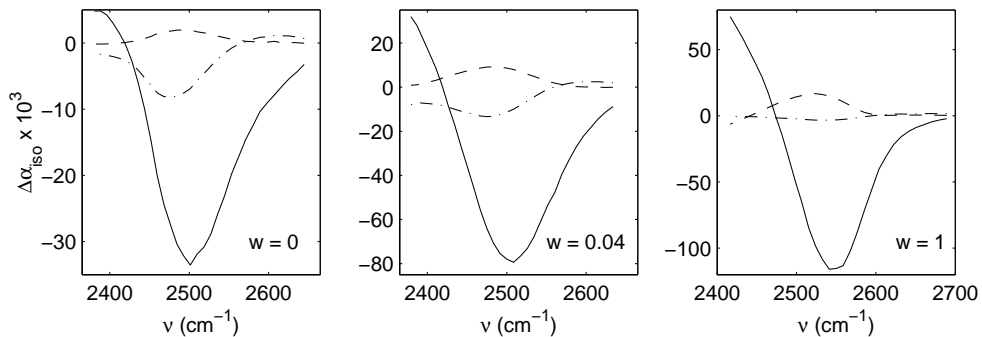


FIG. 7: Decomposition of the transient spectra of TMU-solutions with $w = 0$, $w = 0.04$ and $w = 1$ into the three spectral shapes that follow from the relaxation model. The solid line represents the ground state bleach and excited state absorption. The dashed line is the spectrum of the intermediate state, and the dashed-dotted line corresponds to the heating spectrum.

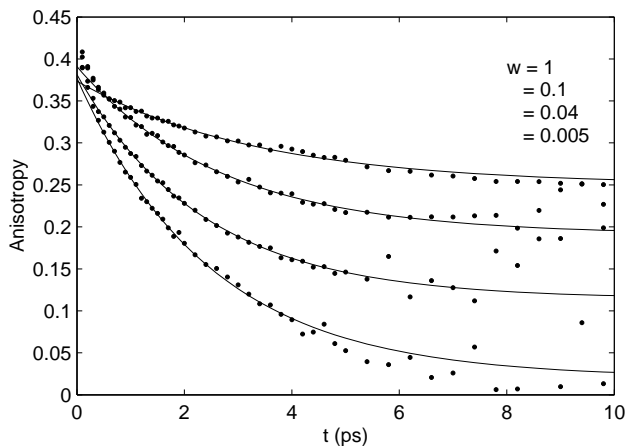


FIG. 8: Anisotropy decay of the OD vibration of HDO in TMU solutions of varying composition. For every solution the probe frequency corresponds to the maximum of the bleach.

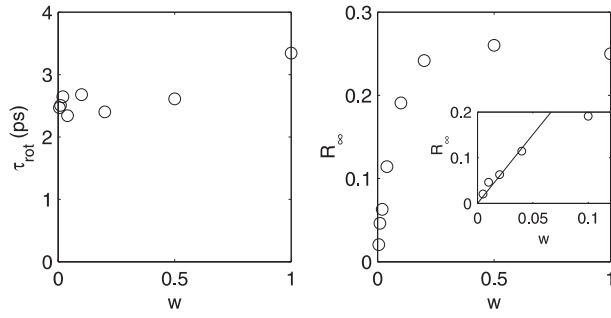


FIG. 9: a) Time constant of the fast component in the anisotropy decay of the OD vibration of HDO as a function of the composition of the solution. The probe frequencies correspond to the center of the absorption bands. b) Amplitude of the slow component in the anisotropy decay as a function of the composition of the solution (same probe frequencies as above). The inset shows the same graph with the x-axis expanded. The solid line represents a linear fit to the first four points.

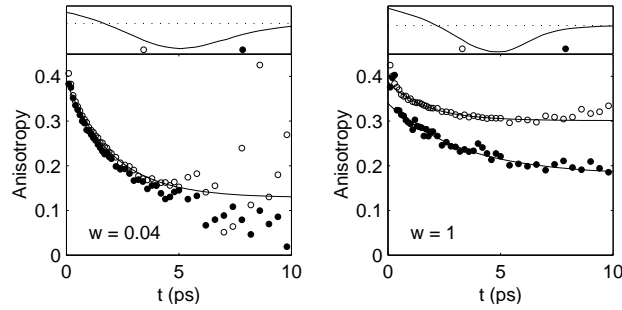


FIG. 10: Dependence of the anisotropy decay on the probe frequency for TMU solutions with $w = 0.04$ (a) and $w = 1$ (b). The solid lines are fits of monoexponentials with an offset. The top panels display the transient spectra, below which the probe frequencies are marked using the symbols from the lower panel.